www.czasopisma.pan.pl PAN POLSKA AKADEMIA NAUK www.journals.pan.pl

A R C H I V E S O F M E T A L L U R G Y A N D M A T E R I A L S

Volume 60 2015 Issue 2

DOI: 10.1515/amm-2015-0248

J. CYRAN*, J. WYRWA*, E. DROŻDŻ*, M. DZIUBANIUK*, M. RĘKAS*,♯

EFFECT OF THE GADOLINIUM OXIDE ADDITION ON THE ELECTRICAL PROPERTIES OF TETRAGONAL ZIRCONIUM DIOXIDE

WPŁYW DODATKU TLENKU GADOLINU NA WŁAŚCIWOŚCI ELEKTRYCZNE TETRAGONALNEGO TLENKU CYRKONU

The aim of this work was examination of gadolinium-doped 3YSZ electrical and structural properties. Such materials may be used as electrolytes in intermediate temperature solid oxide fuel cells (IT-SOFC). First step of the research was synthesis of 3YSZ with different contents of gadolinium (0.25; 0.5; 1.0 at %). Prepared materials were characterized by high porosity. No effect of gadolinium addition on grain size was observed. The experimentally determined values of grain interiors electrical conductivities for gadolinium doped samples are comparable to grain interior conductivities of gadolinium free tetragonal zirconia. On the other hand, a clear effect of gadolinium addition on electrical conductivity of grain boundaries was observed. It was found that 3YSZ containing 0.25 at. % Gd was the most promising from the investigated materials as a solid electrolyte for IT SOFC.

Keywords: Gadolinium (III) oxide, tetragonal zirconia, electrical properties, grain boundary conductivity

Celem pracy było zbadanie strukturalnych i elektrycznych właściwości dwutlenku cyrkonu stabilizowanego 3% mol. tlenkiem itru (3YSZ) z dodatkiem gadolinu. Tego typu materiał może znaleźć zastosowanie jako elektrolit w średniotemperaturowych stało-tlenkowych ogniwach paliwowych (IT-SOFC). Pierwszym etapem badań była synteza 3YSZ z różną ilością wprowadzonego gadolinu (0.25; 0.5; 1.0 at %). Otrzymane materiały charakteryzowały się wysoką porowatością. Nie zaobserwowano wpływu dodatku gadolinu na wielkość ziaren. Wyznaczone eksperymentalnie wartości przewodnictwa objętości ziaren są porównywalne z wartością przewodnictwa objętości ziaren wykazywanego przez czysty 3YSZ (bez dodatku gadolinu). Z drugiej strony, zaobserwowano znaczny wpływ dodatku gadolinu na przewodnictwo po granicach ziaren. Stwierdzono również, że 3YSZ zawierający 0.25% at. gadolinu był najbardziej obiecującym z badanych materiałów pod kątem zastosowania jako elektrolit w IT – SOFC.

1. Introduction

Gadolinium (III) oxide (archaically gadolinia) is an inorganic compound with the formula Gd_2O_3. It is one of the most commonly available forms of the gadolinium rare-earth element, derivatives of which are potential contrast agents for magnetic resonance imaging [1]. It is also commonly used as an component of either CeO_2 [2, 3] or ZrO_2 [4-7] based systems. Gd^{3+} ion is the preferred CeO_2 dopant, named as CGO, compared to other rare-earth elements [3]. $Ce_{0.9}Gd_{0.1}O_{1.95}$ doped ceria has a significantly higher oxygen ion conductivity compared to zirconia, at a reduced temperature, making it ideal for use in low and intermediate temperature fuel cells (IT-SOFC) [2 , 8, 9]. However, ceria-based solid electrolyte suffers from reduction of Ce^{4+} to Ce^{3+} at the anode side of the cell. This process induces n-type electronic conductivity, which tends to decrease of the power output of the solid oxide fuel cells due to an internal electrical shorting. One of the possibility to overtake this problem is use of the bi-layered electrolyte composed from stabilized zirconia and CGO layers [10].

Gd_2O_3-ZrO_2 system found several applications such as burnup material in advanced nuclear reactors [4] dielectric films on GaAs-based MOS capacitors [5]; material for thermal barrier coatings (TBCs) in gas turbines or diesel engine parts [6, 7,11]. On the other side, very little information is available in literature about the material application as a solid electrolyte in fuel cells [1].

Zirconia-based materials are the most commonly used electrolytes in high temperature solid oxide fuel cels (SOFCs). Such devices operate in the temperature range of 850-1000°C [12]. Recently SOFCs attracted much attention due to numerous merits i.e. high efficiency of energy conversion to electricity (ca. 70%), fuel flexibility (H_2, CO, natural gas, LPG, etc), high tolerance for trace levels of impurities in the gas stream.

It is worth to mention that SOFCs based on fully yttria stabilized zirconia (ZrO_2+ 8 mol % Y_2O_3) show high efficiency reaching 70%. Regardless of these advantages, their widespread commercial applications are limited due to high operating temperatures. Performance in high temperature requires special material components in the construction

* AGH UNIVERSITY OF SCIENCE AND TECHNOLOGY, FACULTY OF MATERIALS SCIENCE AND CERAMICS, AL. A. MICKIEWICZA 30, 30-059 KRAKÓW, POLAND

♯ Corresponding author: rekas@agh.edu.pl

(e.g. ceramic interconnects) and leads to shorten devices life time.

Taking into account what mentioned above, developing solid oxide fuel cells working at intermediate-temperature (IT-SOFCs) is an extremely topical issue of a great importance. By lowering the temperature of operation, a wider range of materials can be used reducing the costs of fabrication particularly due to substitutions cheaper metal components for expensive ceramic interconnects. Moreover, lower operation temperature provides more rapid start-up and shut-down, reduced corrosion rate of the cells components, improved durability.

Several materials have been proposed as electrolytes in IT-SOFC [13-16]. Basing on literature data [17, 18] as well as own studies [19] tetragonal zirconia: ZrO_2+3 mol % Y_2O_3 (3YSZ) can be promising solid electrolyte in IT-SOFC. Tetragonal zirconia shows excellent mechanical properties, i.e. its mechanical strength exceeds ca. twice the mechanical strength of the cubic phase zirconia [17]. At moderate temperatures below 700°C the grain interior of the tetragonal 3YTZP exhibits higher conductivity (σ_{gi}) than that of cubic 8YSZ zirconia [20]. However, the total ionic conductivity of 3YSZ is lower by a factor of three compared with the 8YSZ due to high contribution of grain boundary resistivity. This phenomena is known as a the blocking effect [21, 22]. The low electrical conductivity of the zirconia tetragonal form is caused by presence of impurities, mainly silica, that segregated on grain boundaries. Many efforts have been made to reduce the blocking effect in tetragonal zirconia. It was found that the alumina added to the zirconia material acts as the silicon scavenger [14, 19, 23].

Basing on the fact, that Gd_2O_3 easily forms silicates with silica [24, 25] we tested Gd_2O_3 dopant serving as a new silica scavenger, which modifies grain boundary properties of tetragonal ZrO_2 stabilized by Y_2O_3.

2. Experimental

2.1. Preparation of 3YSZ-Gd_2O_3 materials

The modified citric method was applied for synthesis of 3YSZ materials with different Gd_2O_3 contents, i.e. 0, 0.25, 0.5 and 1 at. % of Gd. The saturated solutions of yttrium, zirconyl and gadolinium nitrates were mixed in proper ratio in order to obtain 3YSZ-Gd_2O_3 materials. All reagents used were analytically pure (provided by Sigma-Aldrich) and their compositions were analytically verified by classical chemical analysis (weight method). Next, the appropriate amount of citric acid monohydrate (molar ratio 1:1 of citric acid monohydrate, with 5 mol % excess) was added to the nitrate solution. The resulting solution was left for a few hours on a hot plate (around 200±5°C) to evaporate and then was stirred. The final solution turned to gray gel, which afterwards was heated on the burner in air. The prepared powder was ball milled for 6 hrs and then in an attrition grinder for 8 hrs. Disc pellets were pressed and sintered at 800 and 1200°C.

2.2. Microstructure observations

The microstructure of the sintered samples were studied using the SEM technique (SEM – Nova 200 NanoSEM). The energy dispersive X-ray spectrometer (EDS – Oxford Instruments) coupled with scanning electron microscopy was used to determine the chemical composition of the samples. The analysis was focused on gadolinium distribution.

2.3. Determination of the porosity

Porosity of the solid electrolyte used in fuel cells construction is an important parameter. From one side, material used as an electrolyte should be free of open pores to avoid transport of gaseous components through the electrolyte. On the other side, the material used as a component of anode (e.g. anode supported fuel cell) should contain open pores in order to improve three-phase boundary, where electrochemical reactions involving fuel, electrons and oxygen ions takes place.

The total porosity of studied materials was calculated from the geometrical density:

$$p_{total} = \left(1 - \frac{V_{thor}}{V_{geom}}\right) \times 100\% \tag{1}$$

where V_{thor} is a volume of the sample without any porosity:

$$V_{thor} = \frac{m}{\rho_{aYSZ}} \tag{2}$$

where:

p_{total} – total porosity [%],
V_{geom} – real geometric volume [cm^3]
m – mass of the sample [g]
ρ_{3YSZ} – density of the 3YSZ [g/cm^3]

The open porosity was determined by the impregnability method. The sample was immersed in a backer with distilled water. The backer was placed in the vacuum desiccator in order to remove gaseous content from the open pores. Afterwards the sample was removed from the backer and its surface was dried. The open porosity was determined from the equation:

$$p_{open} = \frac{m_{H_2O} - m_{dry}}{\rho_{H_2O}} \tag{3}$$

where:

m_{H2O} – mass of the sample with water [g]
m_{dry} – mass of the dry sample [g]
ρ_{H2O} – density of water [g/cm^3].

2.4. Impedance measurements

Before measurements of impedance, Ag-paste was applied as the electrodes. The impedance spectra were determined in reduced gas atmosphere (90 vol % Ar = 10 vol. % H_2) at 20, 200, 400, 500, 600, 700 and 750°C. The impedance measurements were performed by means of impedance spectroscopy using a computer-controlled Solatron (FRA 1260 and dielectric interface 1294). The impedance spectra were analyzed using the ZPlot software package provided by Solartron. The measurements were carried out with the frequency range of 0.1Hz -1 MHz. The amplitude of the sinusoidal voltage was 10 mV.

3. Results and discussion

SEM images of the 3YSZ+ 0.25 at. % Gd and the 3YSZ+ 1% Gd, sintered at 1200°C during 2 hrs are shown in **Figs 1 and 2,** respectively. Irregular grain agglomerates of the mean size: 148±38 nm and: 160±35 nm were observed for 0.25 at% and 1 at. %, respectively. Chemical analysis performed by EDS technique (**Figs 3 and 4**) revealed presence of high overlapping picks corresponding to Zr and Y elements and much smaller picks coming from oxygen and residual carbon. The picks corresponding to Gd are almost not discernible from the background.

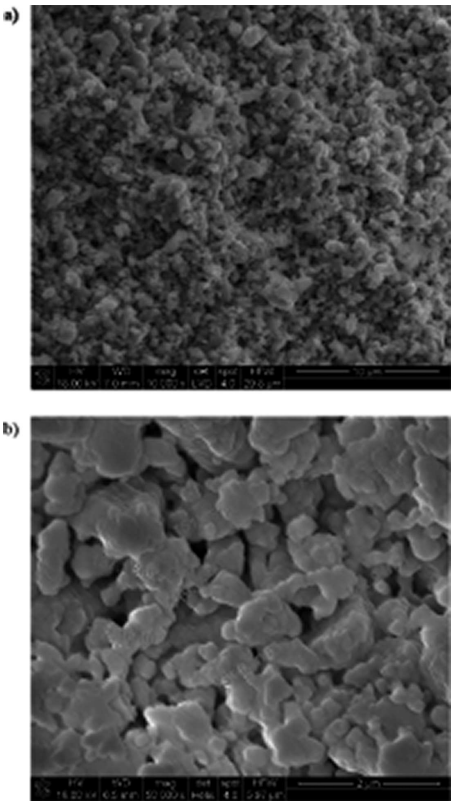

Fig. 1. a, b Typical SEM images of the 3YSZ+0.25 at. % Gd sample

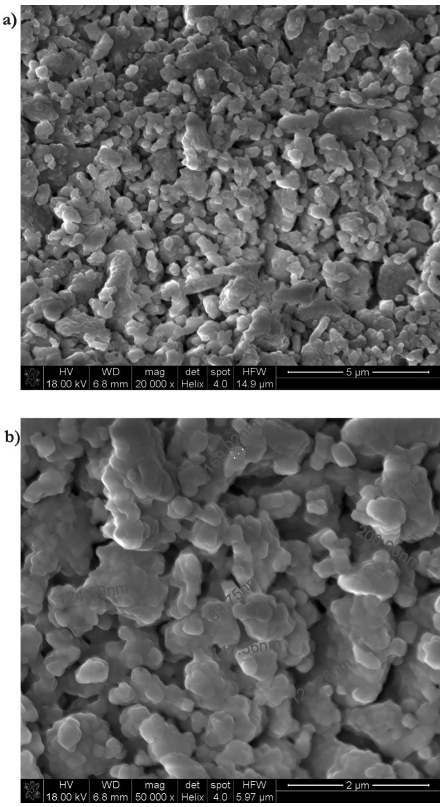

Fig. 2. a, b Typical SEM images 3YSZ+1.0 at. % Gd sample

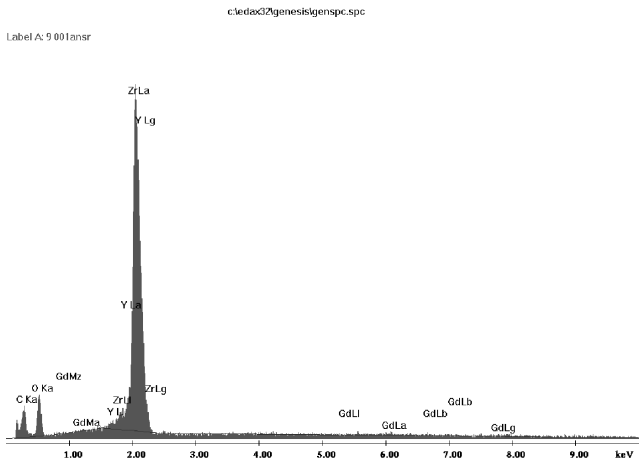

Fig. 3. EDS spectrum of the 3YSZ+0.25 at. % Gd sample

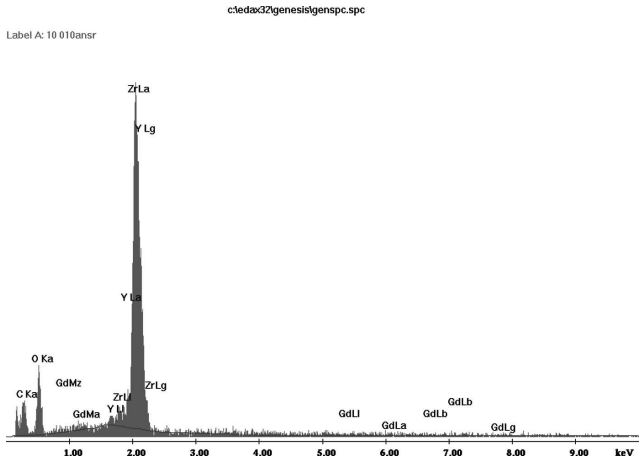

Fig. 4. EDS spectrum of the 3YSZ+1.0 at. % Gd sample

Total and open porosity of the samples sintered at 800°C and 1200°C are schematically presented in **Fig. 5.** For the samples sintered at 800°C estimated values of total and open porosity were: 53.2±0.2% and: 42.9±1.0%, respectively. On the other hand, the values of porosity of the samples, at the same composition, sintered at 1200°C are were: 41.1±2.5% and: 29.1±2.7%, respectively. As can be seen, increasing the sintering temperature leads to decreasing in both total and open porosity.

The experimental Nyquist plots of 3YSZ on the complex impedance plane for 3YSZ and 3YSZ+0.5at % Gd are demonstrated in **Figs 6 and 7,** respectively. The measurements results were presented in the temperature range 500-750°C. One or two parts of semicircles may be distinguished. It is generally accepted [26], that the high-frequency part of the spectrum corresponds to the grain interior (gi) of solid electrolyte, second part (semicircle) is related to a partial blocking of electrical charge (e.g. oxygen ions) at the internal surfaces

of the electrolyte such as grain boundaries (gb), and the third, if any, is attributed to the electrode reactions (el). The idealized impedance spectrum of the ceramic material and corresponding electrical equivalent circuit is schematically shown in **Fig. 8.** R denotes resistors corresponding to resistances of: grain interior (gi), grain boundary (gb) and electrodes (el). CPE is non-Debye element. The impedance Z_{CPE} of the CPE element is described by the formula:

$$Z_{CPE} = \frac{1}{A\,(j\omega)^n} \tag{4}$$

where A and n are fit parameters independent of frequency, j is an imaginary unit and ω is an angular frequency. In particularly, if n = 0.5 or n = 1, the CPE element is named as Warburg element or Debye capacitor, respectively.

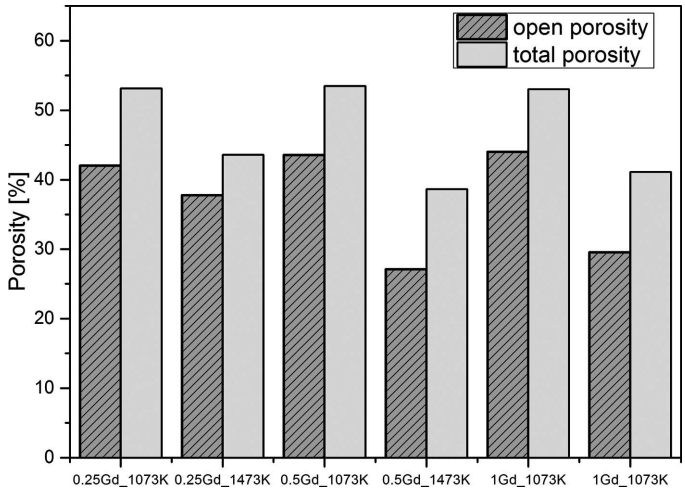

Fig. 5. Total and open porosity of the samples sintered at 800°C and 1200°C

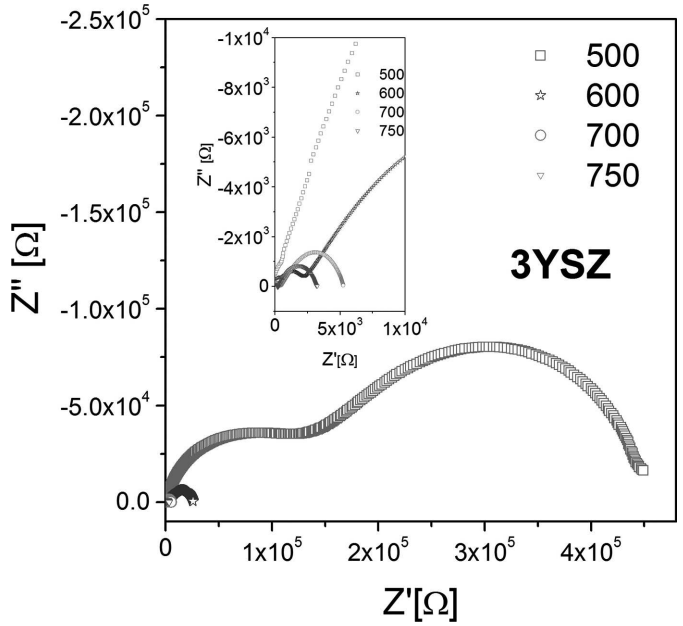

Fig. 6. Nyquist plots of EIS data obtained at four different temperatures for 3YSZ sample

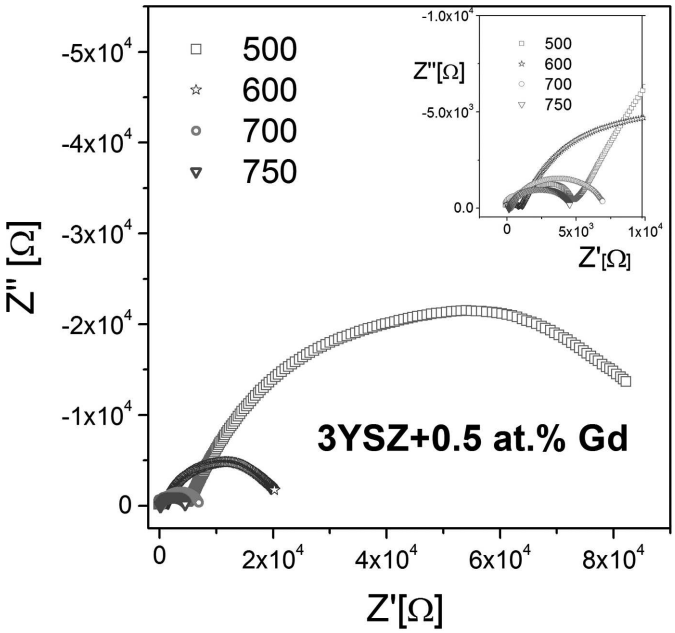

Fig. 7. Nyquist plots of EIS data obtained at four different temperatures for 3YSZ+0.5 at.% Gd sample

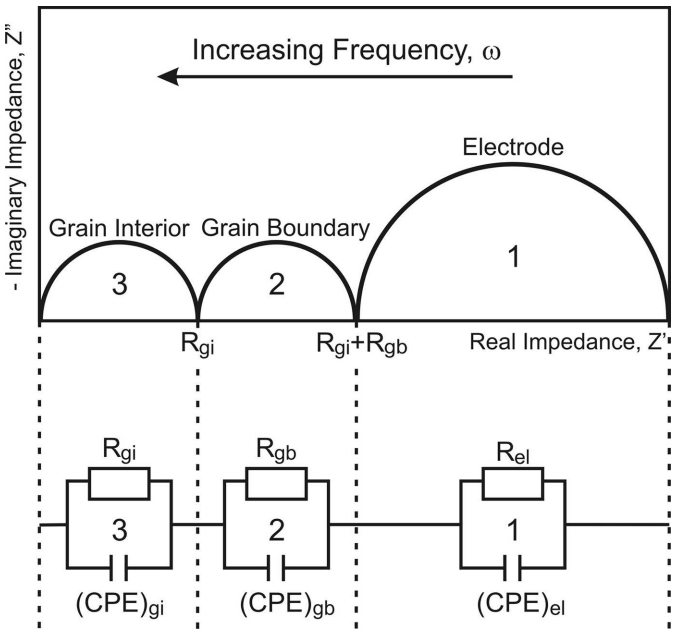

Fig. 8. Equivalent circuit used for fitting of the experimental impedance spectra

A careful analysis of the observed impedance spectra were performed using the equivalent circuit presented in **Fig. 8**. The electrical conductivities of the grain interior, σ_{gi}, and grain boundaries, σ_{gb}, were fitted using the following theoretical (Arrhenius) equation :

$$\sigma T = B \exp\left(-\frac{E_{act}}{RT}\right) \tag{5}$$

where: T – temperature [K], R – gas constant [J/(molK)], E_{act} – activation energy [J]; and B [SK/cm] pre-exponential term, practically independent of temperature. **Figs 9 and 10** illustrate dependencies of log (σT) vs T^{-1} for grain interior and grain boundary, respectively. The linear dependence of σ_{gi} is

observed except the sample containing 1 at % Gd. In the temperature range: 873 -1023K (600-800°C) electrical conductivity of the grain interior (Fig. 9) is characterized by the highest values for concentration of gadolinium 0.25at % and 0.50 at%. On the other hand, within temperature range 773-1023K (500-750°C) or: 873-1023K (600-750°C), the highest values of the electrical conductivity of the grain boundaries were observed for the sample containing 0.25 at % Gd. **Fig. 11** illustrates the dependence of activation energy values of both grain interior and grain boundary conductivities as a function of Gd concentration. The activation energy of grain interior decreases monotonically with Gd content. On the other hand, activation energy of grain interior conductivity shows sharp drop for the sample containing 0.25at % Gd in comparison to undoped sample. Fig. **12** demonstrates electrical conductivity of grain boundaries and grain interiors as a function of gadolinium concentration at 773K (500°C). The conductivity of grain boundaries is practically equal to conductivity of the grain interior for the sample containing 0.25at %. The recorded results indicate, that 0.25 at% Gd is the optimal concentration providing significant improvement of 3YSZ electrical properties.

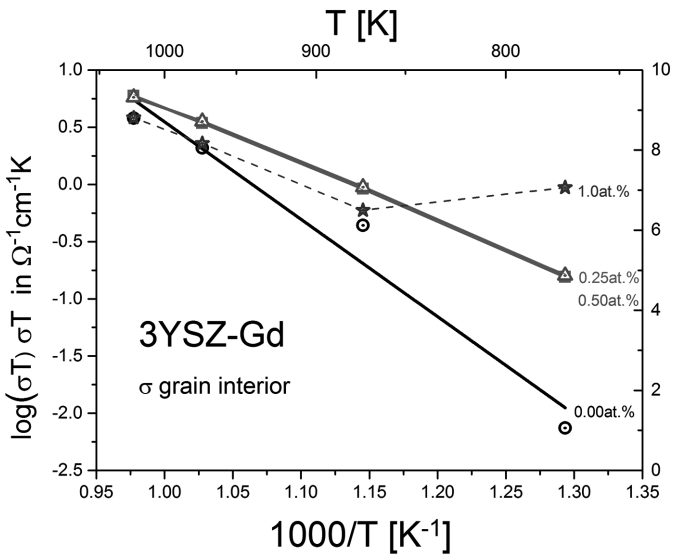

Fig. 9. Arrhenius plot of (σ_{gi}T) for 3YSZ-Gd

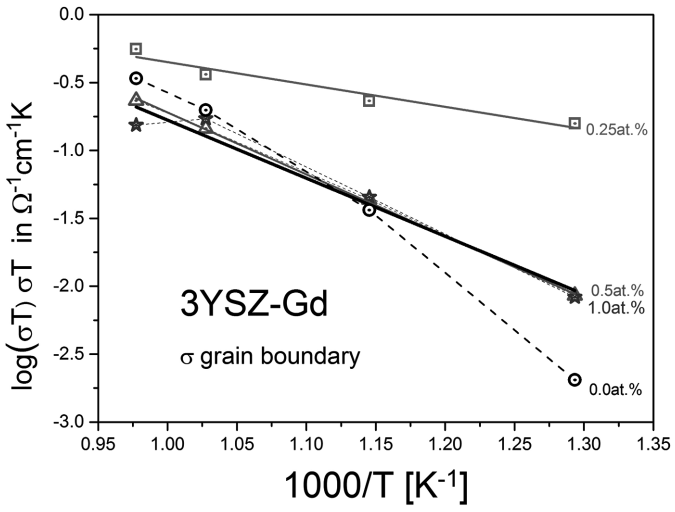

Fig. 10. Arrhenius plot of (σ_{gb}T) for 3YSZ-Gd

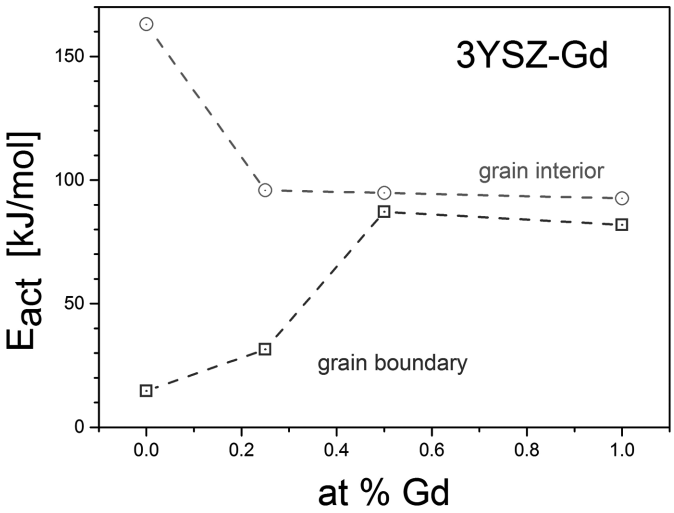

Fig. 11. Activation energy of grain interior and grain boundary electrical conductivity vs. gadolinium concentration

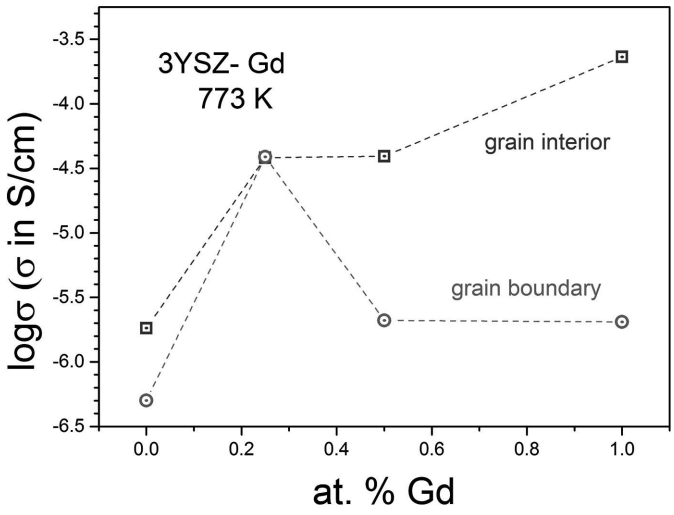

Fig. 12. Electrical conductivity at 773K, as a function of gadolinium concentration

4. Conclusions

The effect of adding different amounts of gadolinium oxide and the influence of sintering temperature on both the microstructure of Gd-doped ZrO_2 containing 3 mol% Y_2O_3 (3YSZ+Gd) and its electrical properties have been studied. The investigation revealed that the 3YSZ sample containing 0.25 mol % Gd_2O_3 showed the most desirable electrical properties from the viewpoint of potential uses as a solid electrolyte in intermediate temperature solid oxide fuel cells (IT-SOFC) constructions.

Acknowledgements

The financial support of the NCN, Grant DEC-2012/05/B/ST8/02723 is gratefully acknowledged.

REFERENCES

[1] K.J. Murphy, J.A. Brunberg, R.H. Cohan, American Journal of Roentgenology **167**, 847 (1996).

[2] B.C.H. Steele, Journal of Power Sources **49**, 1 (1994).
[3] B.C.H. Steele, Solid State Ionics,**129**, 95 (2000).
[4] H. Wang, H. Huang, J.L. Liang, J. Liu, Ceramics International, **40**, 3995 (2014).
[5] Y. Gong, H. Zhal, X. Liu, J. Kong, D. Wu, Applied Surface Science **291**, 35 (2014).
[6] M.N. Rahman, J.R. Gross, R.E. Dultton, H. Wang, Acta Materialia, **54**, 1615 (2006).
[7] A. Portlnha, V. Terelxerla, J. Carneiro, M.F. Costa, N.P. Barradas, A.D. Sequerla, Surface Coating Technology **188-189**, 107 (2004).
[8] M.G. Chourashlya, S.R. Bhardwaj, L.D. Jadhav, Journal of Solid State Electrochemistry **14**, 1869 (2010).
[9] R.J. Ball, R. Stevens, Journal of Materials Science **38**, 1413 (2003).
[10] X. Zhang, M. Robertson, C. Deces-Petit, Y. Xie, R. Hui, I. Qu, O. Kesler, R. Matric, D. Ghosh, Journal of Power Sources **175**, 800 (2008).
[11] D. Shin, H.G. Shin, H. Lee, CALPHAD: Computer Coupling of Phase Diagrams and Thermochemistry **45**, 27 (2014).
[12] R.C. Singhal, K. Kendall, High-Temperature Solid Oxide Fuel Cells: Fundamentals, Design and Applications, Elsevier Sci., Oxford, UK (2005).
[13] S.P.S. Badwal, F.T. Ciacchi, S.S. Rejendran, J. Drennan, Solid State Ionics **109**, 167 (1998).
[14] S.P.S. Badwall, F.T. Ciacchi, Ionics **6**, 1 (2000).
[15] D.J.L. Brett, A. Atkinson, N.P. Brandon, S.J. Skinner, Chemical Society Review **37**, 1568 (2008).
[16] V.V. Kharton, F.M.B. Marques, A. Atkinson, Solid State Ionics **174**, 135 (2004).
[17] S.P.S. Badwal, F.T. Ciacchi, V. Zelizko, Ionics **4**, 25 (1998).
[18] W. Weppner, Solid State Ionics, **52**, 15 (1992).
[19] K. Obal, Z. Pedzich, T. Brylewski, M. Rekas, International Journal of Electrochemical Science **7**, 6831 (2012).
[20] S.P.S. Badwall, J. Drennan, Journal of Matererials Science **24**, 88 (1989).
[21] S.P.S. Badwall, M.V. Swain, Journal of Materials Science Letters **4**, 487 (1985).
[22] D. Meyer, U. Eisele, Ratet, Scripta Materialia **58**, 215 (2008).
[23] M.C. Martin, M.L. Mecartney, Solid State Ionics **161**, 67 (2003).
[24] C-C. Huang, W. Huang, C-H. Su, C-N. Feng, W-S. Kuo, C-S. Yeh, Chemical Communitations 3360 (2009).
[25] J.A. Gupta, D. Landheer, J.P. Mc Caffrey, G.I. Sproule, Applied Physics Letters **78**, 1718 (2001).
[26] J.E. Bauerle, Journal of Physical Chemistry of Solids **30**, 2657 (1969).

Received: 20 February 2014.